molecules

MDPI

Article

Natural-Product-Inspired Microwave-Assisted Synthesis of Novel Spirooxindoles as Antileishmanial Agents: Synthesis, Stereochemical Assignment, Bioevaluation, SAR, and Molecular Docking Studies

Nawal Kishore Sahu [1,2,†], Ritu Sharma [1,†], Kshirsagar Prasad Suhas [3], Jyoti Joshi [4], Kunal Prakash [5], Richa Sharma [1], Ramendra Pratap [5], Xiwen Hu [6], Sukhbir Kaur [4], Mukesh Jain [1], Carmine Coluccini [7,*], Paolo Coghi [6,*] and Sandeep Chaudhary [1,3,*]

1 Laboratory of Organic and Medicinal Chemistry (OMC Lab), Department of Chemistry, Malaviya National Institute of Technology, Jawaharlal Nehru Marg, Jaipur 302017, India; nawal.chemistry@gmail.com (N.K.S.); rtsharma312@gmail.com (R.S.); richasharmachem1@gmail.com (R.S.); mjain.chy@mnit.ac.in (M.J.)
2 Department of Chemistry, Government Engineering College, Bharatpur 321303, India
3 Department of Medicinal Chemistry, National Institute of Pharmaceutical Education and Research, Raebareli (NIPER-R), New Transit Campus, Bijnor-Sisendi Road, Sarojini Nagar, Near CRPF Base Camp, Lucknow 226002, India; kshirsagarprasad06@gmail.com
4 Parasitology Laboratory, Department of Zoology, Panjab University, Chandigarh 160014, India; jyotijoshi86@gmail.com (J.J.); puzoology@yahoo.com (S.K.)
5 Department of Chemistry, University of Delhi, North Campus, Delhi 110007, India; kunp93@gmail.com (K.P.); ramendrapratap@gmail.com (R.P.)
6 School of Pharmacy, Macau University of Science and Technology, Avenida Wai Long, Taipa, Macau, China; 1909853vpa11003@student.must.edu.mo
7 Institute of New Drug Development, College of Medicine, China Medical University, No. 91, Hsueh-Shih Road, Taichung 40402, Taiwan
* Correspondence: carmine.coluccini@mail.cmu.edu.tw (C.C.); coghips@must.edu.mo (P.C.); schaudhary.chy@mnit.ac.in or schaudhary.chy@niperraebareli.edu.in (S.C.); Tel.: +91-141-2713319 or +91-522-2975587 (S.C.); Fax: +91-141-2529029 (S.C.)
† These authors contributed equally to this work.

check for updates

Citation: Sahu, N.K.; Sharma, R.; Suhas, K.P.; Joshi, J.; Prakash, K.; Sharma, R.; Pratap, R.; Hu, X.; Kaur, S.; Jain, M.; et al. Natural-Product-Inspired Microwave-Assisted Synthesis of Novel Spirooxindoles as Antileishmanial Agents: Synthesis, Stereochemical Assignment, Bioevaluation, SAR, and Molecular Docking Studies. *Molecules* **2023**, *28*, 4817. https://doi.org/10.3390/molecules28124817

Academic Editors: Anna Bogucka-Kocka, Przemysław Kołodziej, Monika Wujec, Roman Lesyk and Jacek Bogucki

Received: 1 May 2023
Revised: 12 June 2023
Accepted: 14 June 2023
Published: 16 June 2023

Abstract: Leishmaniasis is a neglected tropical disease, and there is an emerging need for the development of effective drugs to treat it. To identify novel compounds with antileishmanial properties, a novel series of functionalized spiro[indoline-3,2′-pyrrolidin]-2-one/spiro[indoline-3,3′-pyrrolizin]-2-one **23a–f**, **24a–f**, and **25a–g** were prepared from natural-product-inspired pharmaceutically privileged bioactive sub-structures, i.e., isatins **20a–h**, various substituted chalcones **21a–f**, and **22a–c** amino acids, via 1,3-dipolar cycloaddition reactions in MeOH at 80 °C using a microwave-assisted approach. Compared to traditional methods, microwave-assisted synthesis produces higher yields and better quality, and it takes less time. We report here the in vitro antileishmanial activity against *Leishmania donovani* and SAR studies. The analogues **24a**, **24e**, **24f**, and **25d** were found to be the most active compounds of the series and showed IC_{50} values of 2.43 µM, 0.96 µM, 1.62 µM, and 3.55 µM, respectively, compared to the standard reference drug Amphotericin B (IC_{50} = 0.060 µM). All compounds were assessed for Leishmania DNA topoisomerase type IB inhibition activity using the standard drug Camptothecin, and **24a**, **24e**, **24f**, and **25d** showed potential results. In order to further validate the experimental results and gain a deeper understanding of the binding manner of such compounds, molecular docking studies were also performed. The stereochemistry of the novel functionalized spirooxindole derivatives was confirmed by single-crystal X-ray crystallography studies.

Keywords: microwave-assisted synthesis; spirooxindole; antileishmanial agents; molecular docking studies; structure–activity relationship

1. Introduction

According to the World Health Organization (WHO), in 2021, leishmaniasis emerged as an endemic in 99 countries/territories (out of 200 countries/territories), mainly in 4 eco-epidemiological provinces worldwide (the Americas, East Africa, North Africa, and West and South East Asia) [1,2]. It is caused by Leishmania, a protozoan parasite from the Trypanosomatidae family, which is transmitted by vectors and causes cutaneous leishmaniasis (CL), mucocutaneous leishmaniasis (MCL), and visceral leishmaniasis (VL); these are characterized by skin ulcers affecting the mouth, nose, and throat and "kala-azar", respectively [3]. Kala-azar (visceral leishmaniasis) is the fatal form of the disease and is triggered by *Leishmania donovani*, an intramacrophage protozoan parasite transmitted by the bite of infected female phlebotomine sandflies. This lethal disease affects millions of individuals living in tropical/subtropical regions worldwide [4]. Approximately, twenty-one protozoan parasite species of Leishmania are responsible for causing leishmaniasis, and this is linked to a variety of symptomatology ranging from minor skin lesions at the bite site to the deadly visceral forms. A few standard drugs are available for the treatment of this disease, such as pentavalent antimonials, amphotericin B, its liposomal encapsulation (lamb-liposomal amphotericin B), and miltefosine. Amphotericin B emerged as an alternative second-line treatment for visceral, mucocutaneous, and cutaneous leishmaniasis, especially in the case of human HIV coinfection after resistance was reported in antimonials. In Thailand, amphotericin B is the only effective drug available for the treatment of leishmaniasis [5]. According to published research, there is no current safe and effective treatment for leishmaniasis. The antileishmanial medicines used to treat leishmaniasis at present are accompanied by various kinds of side effects, toxicity, and drug resistance [6,7]. As per the WHO report, approximately 700,000 to 1,000,000 new cases are reported every year [8]. Therefore, there is an urgent need for the advent of effective medications against this neglected tropical disease (NTD).

The spirooxindole class of bio-heterocycles are identified as privileged molecules and construct the core structural unit in several naturally occurring alkaloids such as horsfiline **1** [9,10], coerulescine **2** [11,12], marcfortine B **3** [13], spirotryprostatin A **4** and B **5** [14,15], elacomine **6** [16], formosanine **7** [17], pteropodine **8** [18], alstonisine **9** [19], rychnophyilline **10** [20], strychnofoline **11** [21], spirobrassinin **12** [22], mitraphylline **13** [23], notoamide A **14** [24], etc. (Figure 1). Spirooxindoles are blended with a wide range of biological activities such as antimicrobial [25,26], antimigraine activity [27], antitumoral [28], anti-inflammatory [29], antihelmintic activity [30], antimycobacterial [31], acetyl-cholinesterase inhibitory activities [32,33], anticancer activities [34–36], anesthetic [37], HIV-1 N-NRT inhibitor [38], antileishmanial [39], etc.

It has been well-documented that several pharmacologically privileged molecules can be assembled into a single structurally complex molecule with more multi-faceted and enhanced biological activities that can target biological sites of interest in a specific manner to combat specific diseases [40,41]. Several biologically active alkaloidal classes of heterocycles have been reported in the literature and show promising antileishmanial activity in vitro, ex vivo, and in vivo [42–45]. Recent studies have revealed that several substituted spirooxindoles **15**–**19** [46–49] show promising antileishmanial activity against promastigotes and the amastigotes forms of *Leishmania* (L.) species either in vitro or in vivo when treated with pentamidine, amphotericin B, or miltefosine as one of the standard drugs. Therefore, in our endeavor to search for novel bio-heterocycles as antileishmanial agents, we designed Prototype A, i.e., functionalized spiro[indoline-3,2′-pyrrolidin]-2-one/spiro[indoline-3,3′-pyrrolizin]-2-one incorporating subunits of **15**–**19** (Figure 2), and we assessed in vitro antileishmanial activities against the promastigotes form of L. donovani, with the expectation that a new series of amino-acid-based spirooxindole derivatives would also show promising in vitro activity. So far, a literature review has revealed that there is no report available showing amino-acid-based spirooxindoles as antileishmanial agents.

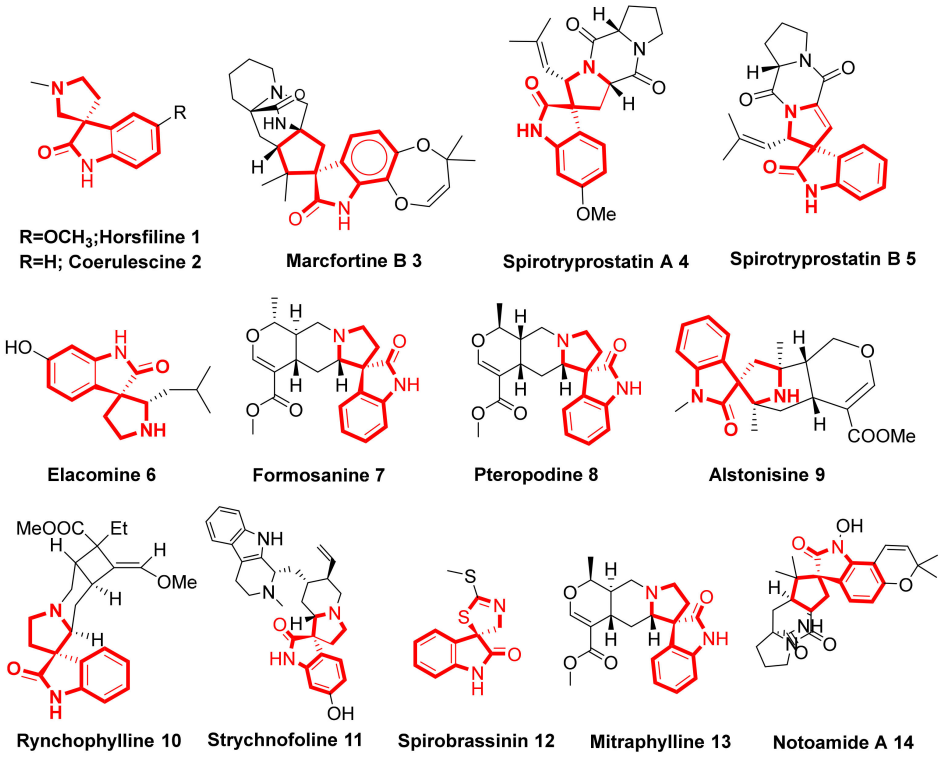

Figure 1. Structures of natural-product-inspired spirooxindole alkaloids **1–14**.

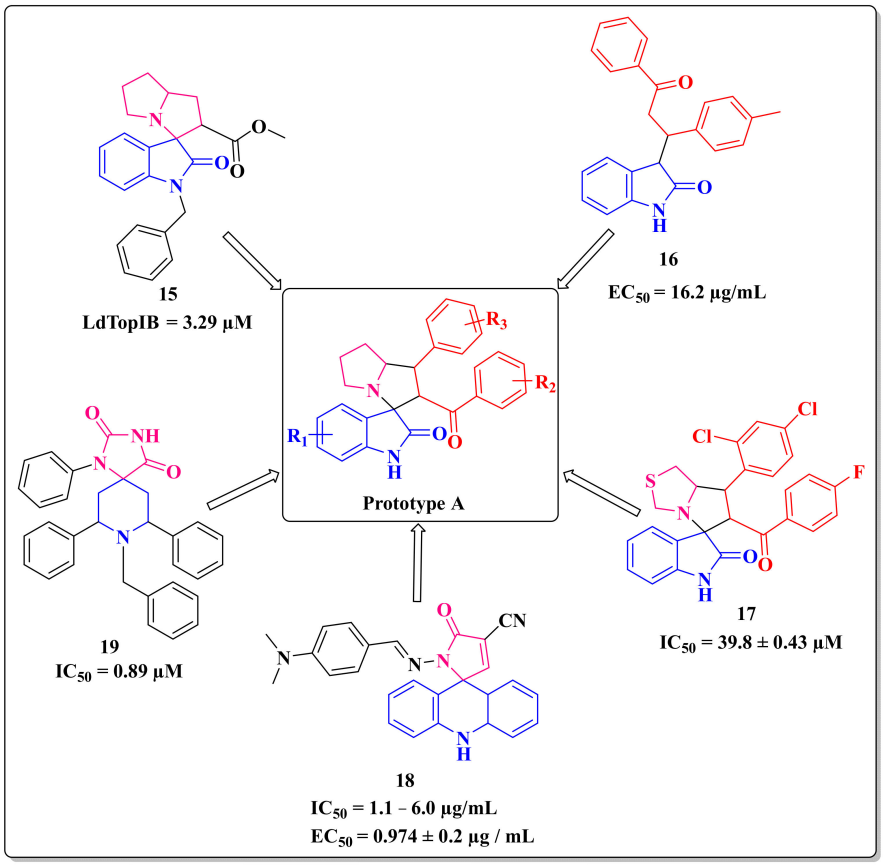

Figure 2. Design strategy for the target functionalized spiro[indoline-3,2′-pyrrolidin]-2-one/spiro[indoline-3,3′-pyrrolizin]-2-one having antileishmanial activity.

Microwave-assisted organic synthesis (MAOS) is a non-conventional, eco-friendly source of energy in chemical synthesis that can perform the reaction in a shorter time with less energy and furnish the product in a greater yield with higher purities as compared to traditional synthetic processes [50–55]. This fascinating method has a wide range of applications in drug discovery evaluation and the pharmaceutical segment for chemical synthesis. It has established an ongoing position in analytical and organic laboratory praxis [56]. Multi-component reactions (MCRs) via 1,3-dipolar cycloaddition reactions have been considered the best potential way for the synthesis of a library of spirooxindole derivatives [57,58].

Herein, we report the microwave-assisted synthesis as well as in vitro antileishmanial activity and structure–activity relationship studies of a novel series of functionalized spiro[indoline-3,2′-pyrrolidin]-2-one/spiro[indoline-3,3′-pyrrolizin]-2-one **23a–f**, **24a–f**, and **25a–g** via 1,3-dipolar cycloaddition. This was achieved by the interaction of various isatins and amino acids with substituted chalcones in up to 98% yields in a highly regioselective and stereoselective manner. For the first time, all the compounds **23a–f**, **24a–f**, and **25a–g** were prepared via microwave-assisted methodology. The stereochemistry of the novel functionalized spiro[indoline-3,2′-pyrrolidin]-2-one/spiro[indoline-3,3′-pyrrolizin]-2-ones was confirmed by single-crystal X-ray crystallography studies of the bromo derivative, i.e., compound **23f**. To the best of our knowledge, functionalized spiro[indoline-3,2′-pyrrolidin]-2-one/spiro[indoline-3,3′-pyrrolizin]-2-one **23a–f**, **24a–f**, and **25a–g** were identified for the first time as promising antileishmanial agents. In this study, amphotericin B was used as the standard reference drug. We also report the validation of wet results via in silico molecular docking studies of active compounds **24a**, **24e**, **24f**, and **25d**.

2. Results

2.1. Synthesis

The 1,3-dipolar cycloaddition reaction of azomethine ylides is a versatile reaction and is well known for the assembly of numerous varieties of complex bioactive azaheterocyclic skeletons [59–61]. The azomethine ylide is also reported to serve as an important building block for the construction of several natural-product-inspired aza-heterocycles [62–64] and bioactive molecules [65].

We commenced our synthetic investigation by taking isatin **20a**, chalcone **21a**, and L-proline **22a** as starting materials for carrying out microwave-assisted synthesis of spirooxindole-pyrrolidine **23a**. Initially, the reaction was attempted under refluxing conditions. Therefore, the reaction was carried out by taking **20a** (1 equiv.), **21a** (1 equiv.), and **22a** (1 equiv.) in MeOH under refluxing conditions for 120 min. We were delighted to get the desired spiro compound **23a** in 86% yield (Table 1, entry 1). Then, we analysed the effect of the number of equivalents of the starting materials. Thus, the reaction was repeated in MeOH with **20a** (1 equiv.), **21a** (1.5 equiv.), and **22a** (1.5 equiv.) under refluxing conditions for 180 min, yielding **23a** in 96% yield (Table 1, entry 2). It was noticed that changing the number of equivalents led to an improvement in the yield of the reaction. In order to reduce the time to complete the reaction, the reaction was subjected exactly to the same conditions as mentioned in entry no. 2 and allowed to run for 120, 60, and 30 min, which produced **23a** in 89%, 67%, and 58% yields, respectively (Table 1, entries 3–5). Keeping the reaction exactly under the same conditions as mentioned in entry no. 2, the screening of different solvents (AcCN, ethylene glycol, H_2O, and ethanol) did not show an incremental effect on the yield of the reaction (Table 1, entries 6–9).

It is well known that microwave irradiation has been used as a fundamental tool for constructing aza-heterocycles with interesting properties, either in homogeneous or heterogeneous liquid reaction systems [66]. Utilizing the dual potential of both microwave irradiation as well as the 1,3,-dipolar cycloaddition reaction strategy; equimolar amounts of **20a** (1 equiv.), **21a** (1.5 equiv.), and **22a** (1.5 equiv.) dissolved in MeOH were treated under microwave irradiation conditions at 80 °C for 1 and 3 min, which produced **23a** in 41% and 71% yield, respectively (Table 1, entries 10–11). Intriguingly, when the same reaction was

subjected to 5 min under microwave conditions; **23a** was obtained in 98% yield (Table 1, entry 12). The reactions were further screened with different solvents (AcCN, ethylene glycol, and ethanol) utilizing the same conditions as mentioned in entry no. 12 with varying times and temperatures (Table 1, entries 13–21). However, none of the reactions produced better yields than those obtained in entry no. 12. Therefore, equimolar amounts of **20a** (1 equiv.), **21a** (1.5 equiv.), and **22a** (1.5 equiv.) dissolved in MeOH under microwave irradiation conditions at 80 °C for 5 min was found to be the best optimized reaction condition (Table 1, entry 12).

Table 1. Optimization study: Microwave-assisted synthesis of novel functionalized spiro[indoline-3,2′–pyrrolidin]–2–one/spiro[indoline-3,3′–pyrrolizin]–2–one **23a** from isatin **20a**, chalcone **21a**, and L-proline **22a** as starting materials.

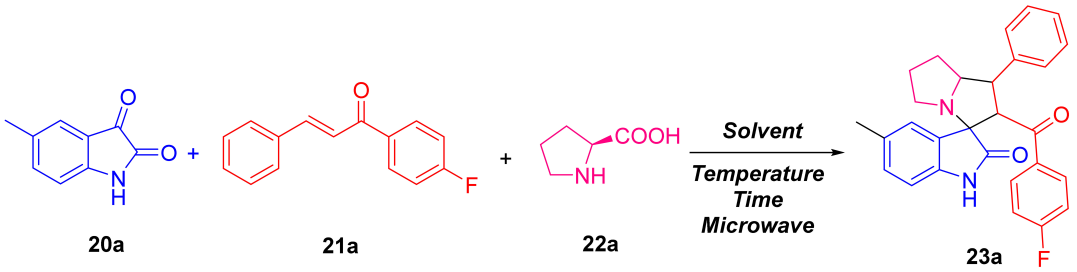

20a 21a 22a 23a

Entry	20a (Eq.)	21a (Eq.)	22a (Eq.)	Solvent	Condition	Time (Min.)	[a] Yield (%)
1.	1	1	1	MeOH	Reflux	120	86
2.	1	1.5	1.5	MeOH	Reflux	180	96
3.	1	1.5	1.5	MeOH	Reflux	120	89
4.	1	1.5	1.5	MeOH	Reflux	60	67
5.	1	1.5	1.5	MeOH	Reflux	30	58
6.	1	1.5	1.5	AcCN	Reflux	180	79
7.	1	1.5	1.5	Ethylene glycol	Reflux	180	76
8.	1	1.5	1.5	H_2O	Reflux	180	9
9.	1	1.5	1.5	Ethanol	Reflux	180	77
10.	1	1.5	1.5	MeOH	MW, 80 °C	1	41
11.	1	1.5	1.5	MeOH	MW, 80 °C	3	71
12.	**1**	**1.5**	**1.5**	**MeOH**	**MW, 80 °C**	**5**	**98**
13.	1	1.5	1.5	AcCN	MW, 80 °C	5	73
14.	1	1.5	1.5	AcCN	MW, 100 °C	10	81
15.	1	1.5	1.5	AcCN	MW, 100 °C	15	83
16.	1	1.5	1.5	Ethylene glycol	MW, 80 °C	5	72
17.	1	1.5	1.5	Ethylene glycol	MW, 100 °C	10	77
18.	1	1.5	1.5	Ethylene glycol	MW, 100 °C	15	79
19.	1	1.5	1.5	Ethanol	MW, 80 °C	5	78
20.	1	1.5	1.5	Ethanol	MW, 100 °C	10	82
21.	1	1.5	1.5	Ethanol	MW, 100 °C	15	85

[a] Isolated yield after recrystallization/column chromatography.

Substituted isatins **20a–h**, substituted chalcones **21a–f**, and various amino acids **22a–c** were subjected to microwave-assisted 1,3-dipolar cycloaddition reactions in MeOH at 80 °C for 5 min, which produced the desired chalcone-isatin-amino-acid-based spirooxindole

compounds **23a–f**, **24a–f**, and **25a–g** in excellent yields (up to 98%) in a highly diastereoselective manner (Scheme 1, Please see Supplementary Materials). In this reaction, [3 + 2] cycloaddition of substituted chalcones occurred with in situ generated azomethine ylides from microwave-assisted decarboxylative condensation of substituted isatins and various secondary amino acids.

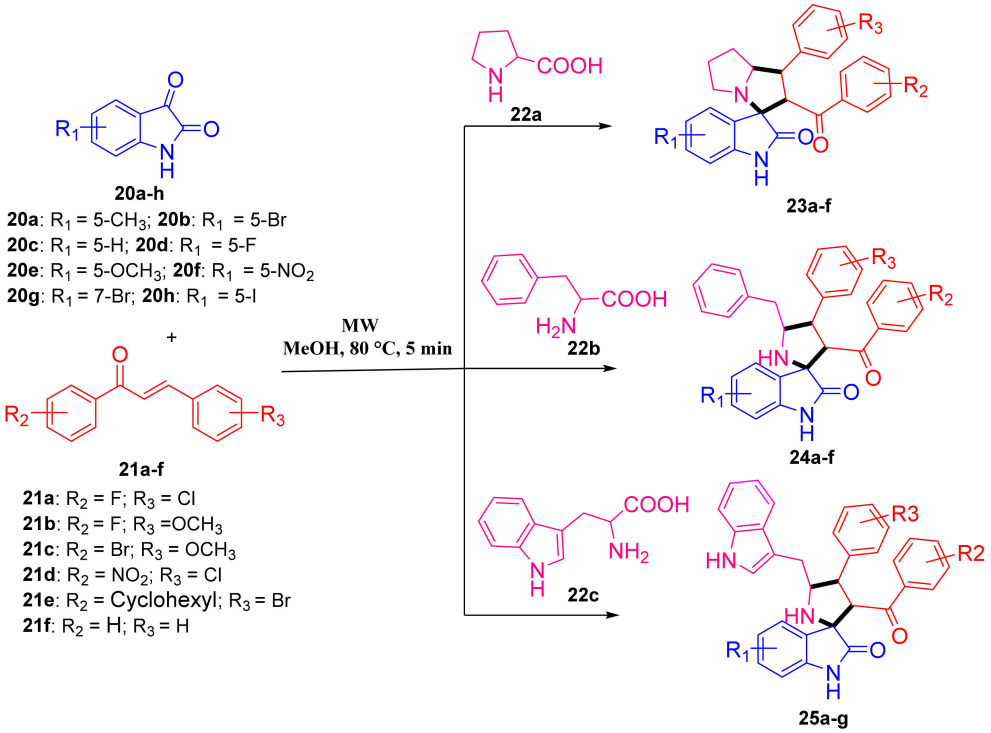

Scheme 1. Microwave-assisted synthesis of novel functionalized spiro[indoline-3,2′-pyrrolidin]-2-one/spiro[indoline-3,3′-pyrrolizin]-2-one **23a–f**, **24a–f**, and **25a–g** via the 1,3-dipolar cycloaddition reaction.

The physico-chemical data, such as melting point and yield, under conventional conditions as well as in microwave-assisted conditions for all the compounds (**23a–f**, **24a–f**, and **25a–g**) are shown in Table 2.

The structures of all the synthesized compounds were well characterized by FT-IR, optical rotation, ^{1}H-NMR, ^{13}C-NMR spectroscopy, and HRMS mass spectrometric analysis (Please see Supplementary Materials). Finally, the stereochemistry of the four chiral centres of the cycloaddition reaction was unequivocally determined by single-crystal X-ray diffraction analysis of the cycloadduct **23f** (Figure 3, please see Supplementary Materials). After screening over the series of other derivatives, we found that the **23f** prepared in one step and obtained as an off-white solid in 86% yield, which was further subjected to crystallization; we were able to isolate the **23f** in ~10–11% yield using a slow evaporation crystallization technique with DCM as a solvent at low temperature. After couple of weeks, we came up with the single-crystal X-ray structure of the **23f**, the raw data of **23f** were subjected to the solution using Olex2 [67], and the crystal was crystallized in a trigonal system in R-3 space group. Consequently, the three-dimensional representation of compound **23f** shows that the compound has four chiral carbons, with one carbon having an R-configuration and the other three having S-configurations. The crystal structure confirmed that the trans-geometry of chalcone and the regioselectivity were also well established as a result of the concerted reaction of chalcones with the ylides.

Table 2. Physicochemical data of spirooxindole pyrrolidines/pyrrolizines compounds **23a–f**, **24a–f**, and **25a–g**.

Sr. No.	Isatin's (20a–h)	Chalcones (21a–f)		Amino Acids (22a–c)	Product	Reflux (180 Min.)	Microwave Heating (5 Min.)	M.P. (°C)
	R_1	R_2	R_3			Yields [a] (%)	Yields [b] (%)	
1.	5-CH_3	-F	-Cl	**22a**	**23a**	96	98	182–184
2.	5-F	-F	-OCH_3	**22a**	**23b**	61	72	161–163
3.	5-F	-Br	-OCH_3	**22a**	**23c**	59	74	126–128
4.	5-OCH_3	-Br	-OCH_3	**22a**	**23d**	82	93	107–109
5.	5-NO_2	-Br	-OCH_3	**22a**	**23e**	72	83	111–113
6.	5-Br	-H	-H	**22a**	**23f**	71	86	175–177
7.	5-OCH_3	-NO_2	-Cl	**22b**	**24a**	75	89	188–190
8.	5-NO_2	-CH_3	-Br	**22b**	**24b**	82	95	121–122
9.	5-CH_3	-NO_2	-Cl	**22b**	**24c**	79	88	135–137
10.	5-H	-F	-Cl	**22b**	**24d**	89	97	104–106
11.	5-Br	-NO_2	-Cl	**22b**	**24e**	69	83	166–168
12.	7-I	-CH_3	-Br	**22b**	**24f**	96	98	101–102
13.	5-Br	-F	-OCH_3	**22c**	**25a**	81	91	154–156
14.	5-H	-Br	-OCH_3	**22c**	**25b**	61	75	118–120
15.	5-Br	-F	-Cl	**22c**	**25c**	63	71	138–140
16.	5-F	-Cyclohexyl	-Br	**22c**	**25d**	57	73	112–114
17.	5-CH_3	-F	-OCH_3	**22c**	**25e**	74	87	103–105
18.	5-NO_2	-F	-Cl	**22c**	**25f**	58	72	172–174
19.	5-OCH_3	-F	-Cl	**22c**	**25g**	67	81	142–144

[a] Isolated yields by column chromatography (conventional method). [b] Isolated yields by column chromatography (microwave-assisted synthesis).

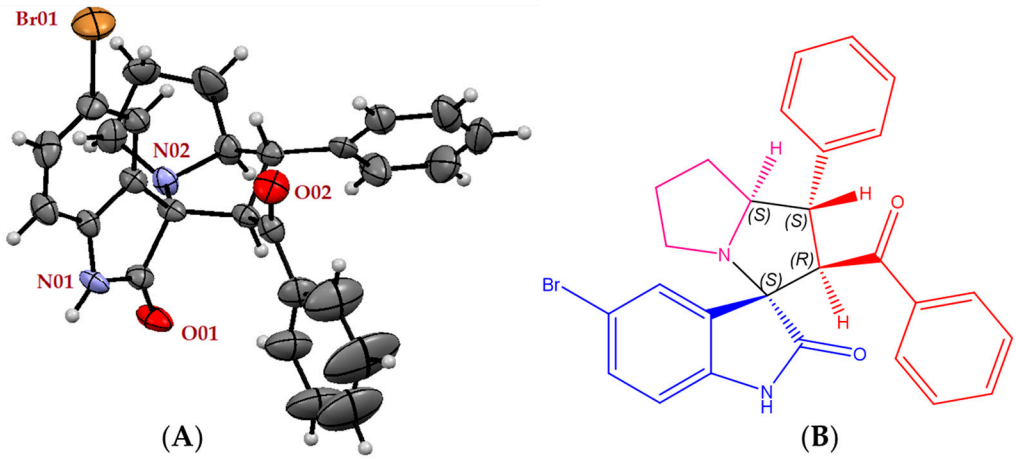

Figure 3. (**A**) ORTEP diagram of the cycloadduct **23f**. (**B**) Structure of (1′S,2′R,3S,7a′S)-2′-benzoyl -5-bromo-1′-phenyl-1′,2′,5′,6′,7′,7a′-hexahydrospiro[indolin-3,3′-pyrrolizin]-2-one **23f**.

2.2. Single-Crystal X-ray

Furthermore, it was observed that the crystallized framework had a hexagonal architecture consisting of six molecules in a circular fashion around the disordered functionality that takes non-planar circular conformations with the presence of short contacts in the alternate configuration. The molecular arrangement of **23f**, its inside functionality in a large

cavity, and its size are directly proportional to the distance between the carbon atoms at the opposite sides and the Van der Waals radius of the carbon atom present in the ring. In order to understand more about the intermolecular interactions of **23f**, a Hirshfeld surface analysis using Crystal Explorer 3.1 software suite was used [68]. The 3D representation of short intermolecular contact can be provided by de and di mapped on the Hirshfeld surface, which corresponds to exterior and interior distances, respectively. The d_{norm}, shape index, and curvedness of **23f** roughly indicating the presence of strong intermolecular short contacts and stronger Van der Waals interactions. The 2D finger plot of **23f** reveals significant interactions corresponding to C-C, H-C, and H-H contributes 4.5%, 8.9%, and 39.0% of the total Hirshfeld surface, respectively, which is again attributable to the presence of strong intermolecular interactions; these are more prominent that of π–π interactions (Figure 4).

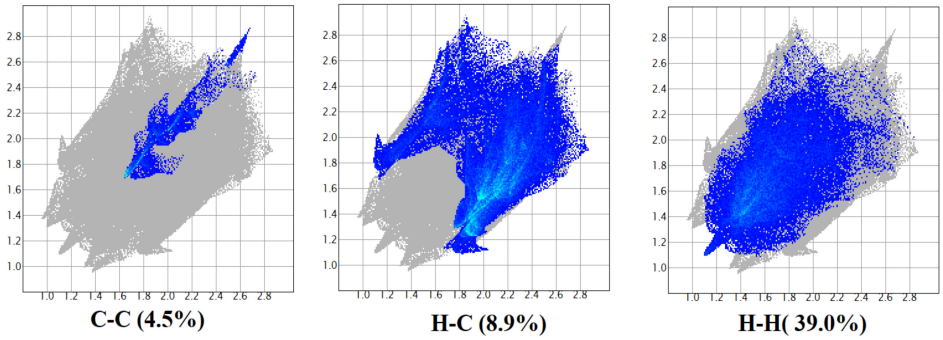

Figure 4. The 2D Finger plot of C-C, H-C, and H-H of **23f**.

As can be seen from Scheme 1 and Figure 4, all synthesized spirooxindoles **23a–f**, **24a–f**, and **25a–g** were obtained in the 71–98% yield range. It was noticed that the reactions were occurring smoothly under microwave conditions with very good to excellent yields; however, the effects of the electron-donating group (EDG) and/or the electron-withdrawing group (EWG) had a marginal influence on the yield of the reaction. Among the spiro[indoline-3,2′-pyrrolidin]-2-one/spiro[indoline-3,3′-pyrrolizin]-2-one derivatives, i.e., **23a–f**, **24a–f**, and **25a–g**, it was noticeable that the EDG (Me, OMe, cycloalkyl, Cl, Br, and I), either on isatin or on Chalcone, produced the desired compound in excellent yield for **23a**, **23d**, **24d**, **24f**, and **25a–b**. However, in the case of EWG (NO_2, F), either on isatin or on chalcone, the target compounds were obtained in a good-to-excellent yield range (Figure 5).

2.3. Biological Activity

Considering the importance of amphotericin B in the control of visceral leishmaniasis, the drug was selected as a control in the present study [69]. Camptothecin, a recognized inhibitor of LTopIB, effectively inhibits topoisomerase IB [70].Therefore, both drugs were used as control drugs for performing in vitro antileishmanial activity of all synthesized spirooxindoles **23a–f**, **24a–f**, and **25a–g**.

2.3.1. In Vitro Antileishmanial Activity

The compounds (**23a–f**, **24a–f**, and **25a–g**) were initially screened for their in vitro antileishmanial activity against promastigotes of *Leishmania donovani* (MHOM/IN/1983/AG83) utilizing the Trypan blue dye exclusion method [71] and the plasmid relaxation assay using amphotericin B and camphothesin as standard reference drugs, respectively [72,73].

Trypan Blue Dye Exclusion Method

The promastigotes were harvested from the culture vials, counted, and 2×10^6 cells/well were seeded in a 48-well culture plate. The antileishmanial screening of all the derivatives, **23a–f**, **24a–f**, and **25a–g**, as well as the positive control, was performed at various concentrations (2 µg/mL, 4 µg/mL, 8 µg/mL, and 16 µg/mL) added in triplicate. The plate was

incubated at 22 ± 1 °C in the BOD incubator for 72 h. After 72 h, each well was counted for the number of viable parasites using the Trypan blue dye exclusion method, and the percentage growth inhibition was calculated by using the formula:

$$\text{Percentage viability} = \frac{\text{No. of viable cells in treated well}}{\text{No. of viable cells in blank well}} \times 100$$

$$\text{Percentage growth inhibition} = 100 - \text{percentage viability}$$

The IC_{50} (inhibitory concentration at which 50% of the parasites were dead) value was obtained by plotting a linear dose–response curve in SPSS software (Version 23) [71].

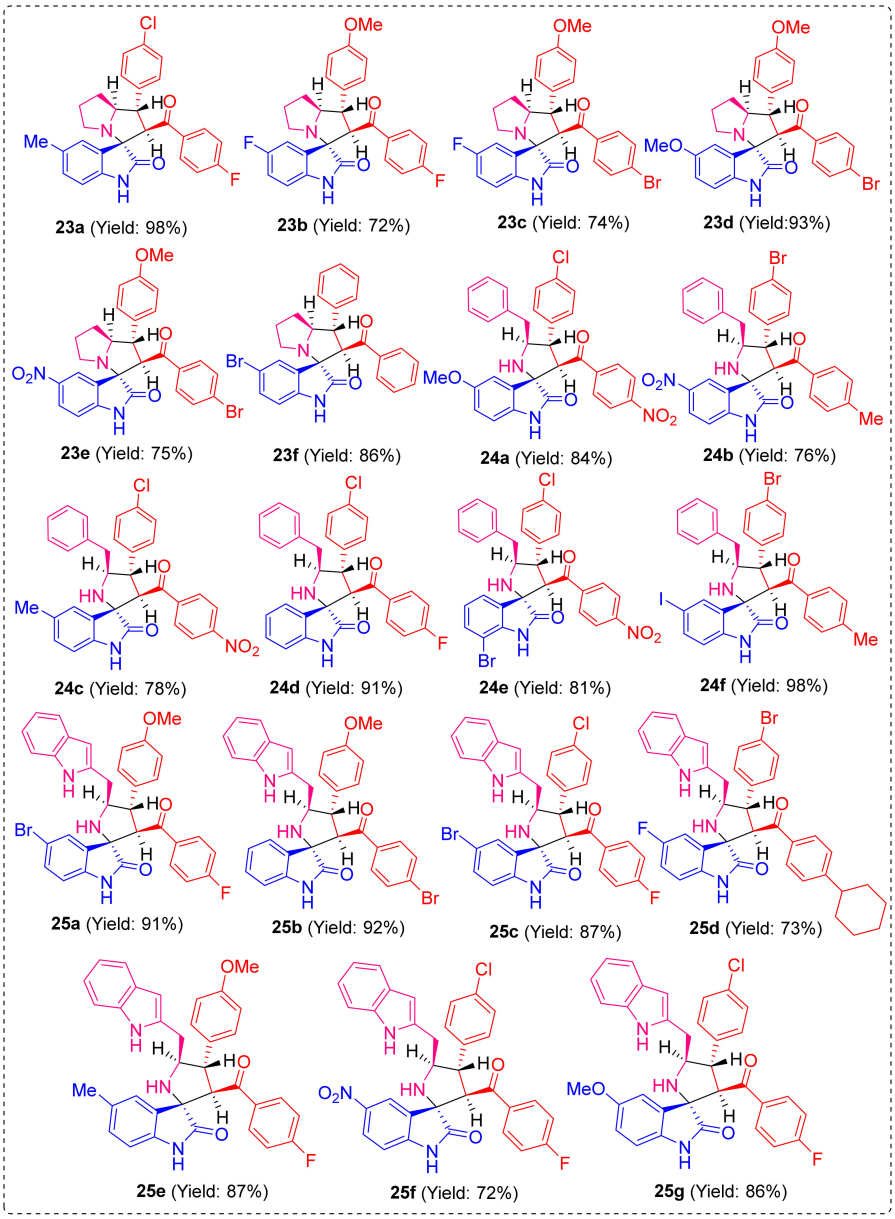

Figure 5. Structures of all synthesized spirooxindoles **23a–f**, **24a–f**, and **25a–g**.

Plasmid Relaxation Assay

The relaxation of supercoiled plasmid DNA is the method used for the determination of LTopIB activity. Various doses of each compound were treated with one unit of pure LTopIB (the enzyme to relax 0.5 µg of supercoiled DNA for 30 min at 37 °C) for 20 min at 4 °C. The reaction mixture, including 0.5 µg of supercoiled pBluescript SK(−) plasmid,

10 mM Tris-HCl buffer pH 7.5, 5 mM $MgCl_2$, 0.1 mM EDTA, 15 µg/mL of bovine serum albumin, and 150 mM KCl, was then added in a final volume of 20 µL. After 30 min at 37 °C, the reaction mixtures were stopped by adding 4 µL of loading buffer, which included 5% sarkosyl, 0.12% bromophenol blue, and 25% glycerol. By electrophoresis, the topoisomers were separated on 1% agarose gels and electrophoresed at 2 V/cm for 16 h in a 0.1 M Tris-borate-EDTA buffer (pH 8.0) after being stained with ethidium bromide (0.5 µg/mL). Plotting the percentage of supercoiled DNA versus drug concentrations allowed researchers to determine the 50% inhibition concentration (IC_{50}) values of LTopIB inhibition as the 50% reduction of supercoiled DNA [72].

2.3.2. Inhibition of Leishmanial DNA Topoisomerase IB

Because of the presence of spirooxindole systems in the structure of these compounds, we aimed to assess their inhibitory potential on purified recombinant LTopIB measuring the relaxation of supercoiled plasmid DNA. In this regard, all spirooxindole derivatives were assessed for LTopIB inhibition through the prevention of DNA relaxation in a circular DNA plasmid. All compounds were tested at a single concentration of 100 µM to discard those that did not prevent DNA relaxation by LTopIB. After this initial test, potential inhibitor dose/response curves were performed to obtain their IC_{50} values. The compounds **24a**, **24e**, **24f**, and **25d** were potent LTopIB inhibitors, and the IC_{50} values of all nineteen compounds are shown in Table 3. The lowest IC_{50} value corresponded to **24e** (IC_{50} = 15.7 µM).

Table 3. In vitro antileishmanial activity of novel functionalized spiro[indoline-3,2′ -pyrrolidin]-2-one/spiro[indoline-3,3′-pyrrolizin]-2-one based compounds **23a–f**, **24a–f**, and **25a–g**.

Spirooxindole Derivatives, i.e., 23a–f, 24a–f, and 25a–g	IC_{50} (µM) [a] Using Trypan Blue Dye Exclusion Method	IC_{50} (µM) [a] Using Plasmid Relaxation Assay
23a	>10 µM	>100 µM
23b	>20 µM	>100 µM
23c	>20 µM	>100 µM
23d	7.78 µM	53.6 µM
23e	>20 µM	>100 µM
23f	>20 µM	>100 µM
24a	**2.43 µM**	**17.3 µM**
24b	5.36 µM	37.6 µM
24c	>20 µM	>100 µM
24d	>20 µM	>100 µM
24e	**0.96 µM**	**15.7 µM**
24f	**1.62 µM**	**19.6 µM**
25a	>10 µM	71.3 µM
25b	>10 µM	89.1 µM
25c	>10 µM	64.5 µM
25d	**3.55 µM**	**27.2 µM**
25e	>10 µM	>100 µM
25f	>20 µM	>100 µM
25g	>10 µM	78.4 µM
Amphotericin B	**0.060 µM**	-
Camptothecin	-	**3 µM**

[a] IC_{50}: value indicates the effective concentration of a compound required to achieve 50% growth inhibition in µM.

All nineteen compounds exhibited moderate-to-good antileishmanial activity against *Leishmania donovani*. The results are shown in Table 3.

2.3.3. Structure–Activity Relationship (SAR) Studies

The inhibitory concentration (IC) values for all the spiro[indoline-3,2′-pyrrolidin]-2-one/spiro[indoline-3,3′-pyrrolizin]-2-one derivatives, i.e., **23a**–**f**, **24a**–**f**, and **25a**–**g**, and the positive-control drugs, were also determined against promastigotes of *Leishmania donovani* utilizing the Trypan blue dye exclusion method [68]. Amphotericin B was taken as a positive control. As can be seen from Table 3, compound **24e**, the most active compound of the series, showed potent in vitro antileishmanial activity, with the IC_{50} value of 0.96 μM against *Leishmania donovani*. Compound **24f**, the next most active compound in the series (IC_{50} = 1.62 μM), exhibited potent antileishmanial activity in comparison to the standard drug Amphotericin B (IC_{50} = 0.060 μM). Subsequently, compounds **24a** and **25d** also showed promising antileishmanial activity, with IC_{50} values of 2.43 μM and 3.55 μM, respectively. Furthermore, compounds **23d** and **24b** showed moderate activity ($IC_{50} \leq 10$ μM). The rest of the compounds exhibited a lesser activity profile. Thus, SAR experiments indicated that the L-phenylalanine-based spirooxindoles showed a better antileishmanial activity profile as compared to L-proline and L-tryptophan-based counterparts. In proline-based spirooxindoles **23a**–**f**, the EDG group (OMe, Me) on the isatin moiety and the halogen (X = Br) on the chalcone functionality, i.e., **23d**, provided significant activity compared to Amphotericin B. Subsequently, phenylalanine-based spirooxindoles **24a**–**f** were found to be the best active compounds among the series. However, the presence of EDG (OMe, Me), EWG (NO_2, F), or a halogen (X = Br, I) on the isatin moiety showed promising antileishmanial activity in compounds **24a**, **24b**, **24e**, and **24f** despite having EDG, EWG, or halogen groups on chalcone, except **24c**–**d**. Furthermore, among tryptophan-based spirooxindoles **25a**–**g**, the presence of EDG (OMe, Me), EWG (NO_2, F), or a halogen (X = F, Br) on the isatin moiety showed moderate activity (**25d**) despite having EDG (OMe, Me, cyclohexyl), EWG (X = F), or a halogen (X = F, Cl, Br) on chalcone functionality. It was also observed that the presence of EDG or EWG on the spiroskeleton had no influence on the yield of the reaction.

2.4. Molecular Docking Studies

The molecular docking studies of the most active spiro[indoline-3,2′-pyrrolidin]-2-one/spiro[indoline-3,3′-pyrrolizin]-2-one derivatives, i.e., **24a**, **24e**, **24f**, and **25d**, were performed with *Leishmania donovani* topoisomerase I-vanadate-DNA complex protein (PDB ID: 2B9S) using Discovery Studio Visualizer Software [43].

2.4.1. Ligand Preparation

The two-dimensional structure (2d) of novel functionalized spiro[indoline-3,2′-pyrrolidin]-2-one/spiro[indoline-3,3′-pyrrolizin]-2-one-based compounds **23a**–**f**, **24a**–**f**, and **25a**–**g** along with standard drugs amphotericin and camptothecin were drawn in Chem Draw Ultra 22.0 software, and then the 2D structures of the ligands were converted into MDL molfile V3000 (*mol) format. The ligand was finally optimized with a small molecule protocol, which helps to remove tautomers, isomers, and duplicate conformations.

2.4.2. Protein Preparation

The protein crystal 3D structures of the heterodimeric L. Donovani topoisomerase I- vanadate DNA complex were taken from the protein data bank (PDB), PDB ID 2B9S. The protein was minimized using the simulation protocol via the CHARMm-based smart minimizer method, and protein preparation involved five different steps: cleaning protein, inserting missing atoms, refining loops, minimizing loops, and protonating protein.

2.4.3. In Silico Studies

Analysis of the docking results was carried out by comparing the binding affinities of all the proposed docked molecules to the complex protein. The docking of the abovementioned protein was carried out by removing DNA, and the remaining protein was kept in a grid box. Then, we explored the binding orientation of active functionalized spirooxindoles in terms of their Cdocker energy and Libdock score. It is to be noted that low Cdocker energy and high Libdock score values indicate higher binding affinity toward the target protein, thereby reflecting its higher potency (Table 4).

Table 4. Docking score, i.e., binding energy, of spirooxindole derivatives **24a**, **24e**, **24f**, **25d**, and camptothecin obtained from docking studies.

Compounds	-Cdocker Energy (kcal/mol)	CDocking Interaction Energy (kcal/mol)	Libdock Score
24a	−17.1681	26.9327	128.598
24e	−7.7614	30.2844	96.0439
24f	−7.7800	30.3540	131.125
25d	−14.6475	32.2816	83.1911
Camptothecin	−10.838	30.4772	123.320

The docking results for **24a** against *Leishmania donovani* showed a high binding affinity docking score indicated by a total score of 128.598, and it formed three H-bonds of length 2.19 Å, 2.9 Å, and 2.16 Å to the hydrophobic nucleophilic residues, i.e., the side chains of ASP: A-353 (aspartic acid), ARG: A-190 (arginine), and ASN: B-221 (asparagine), respectively. In the docking pose of the complex, the chemical nature of binding site residues within a radius of 3 Å showed non-bonding Van der Waals interactions with HIS: A-193 (histidine), ARG: A-314 (arginine), THR: B-217 (threonine), ILE: B-220 (isoleucine), and LYS: A-352 (lysine), thus leading to more stability and activity in this compound. In addition, 24a also exhibited a π–anion interaction with ASP: A-353 and an alkyl–π–alkyl interaction with the TYR: B-222 (thyrosine) amino acid residue (Figure 6).

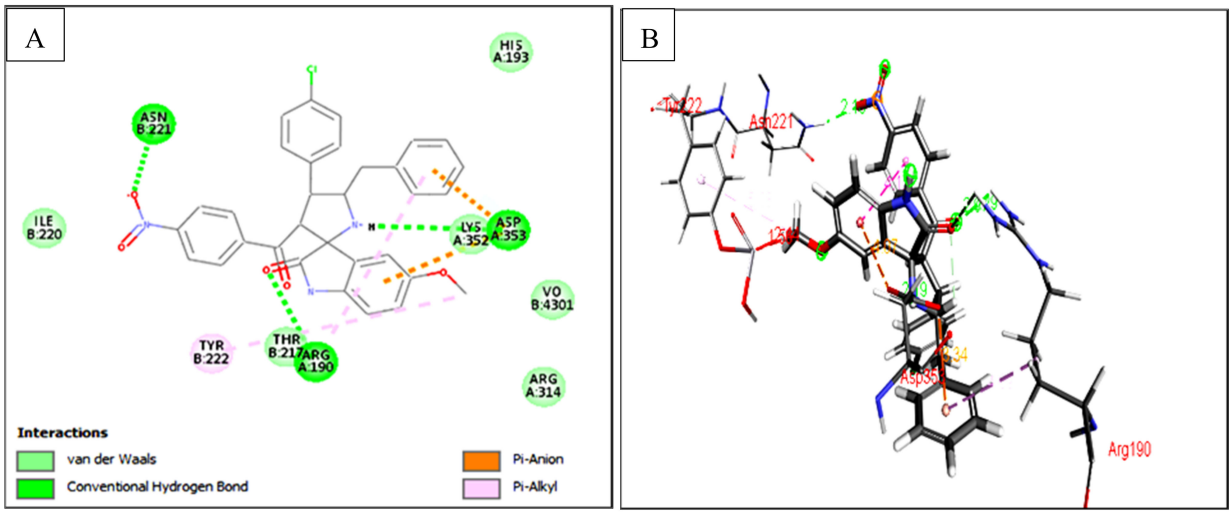

Figure 6. (**A**): Predicted 2D interactions of **24a** with *Leishmania donovani* (PDB ID: 2B9S) with a docking total score of 128.598, revealing H-bonding to the hydrophobic aliphatic residue, i.e., the side chain of LYS: A-352 (lysine). (**B**) Predicted 3D interactions of **24a** with *Leishmania donovani* (PDB ID: 2B9S) with a docking total score of 128.598, revealing π–anion interaction and alkyl–π–alkyl interaction with TYR: B-222 (tyrosine).

The docking results for **24e** against *Leishmania donovani* showed a docking score of 96.0439 and showed attractive charges between nitro group substitution with ASP: A-353 (aspartic acid) and ARG: A-190 (arginine) of bond lengths of 4.58 Å and 3.80 Å, respectively, and LYS: A-352 (lysine) amino acids involved in H-bonds of lengths 2.37 Å and 2.23 Å with the carbonyl oxygen of the ligand. Furthermore, single carbon–hydrogen bond was observed with a bond length of 2.7 Å with ARG: A-190 (arginine), showing the presence of additional H-bonding (Figure 7).

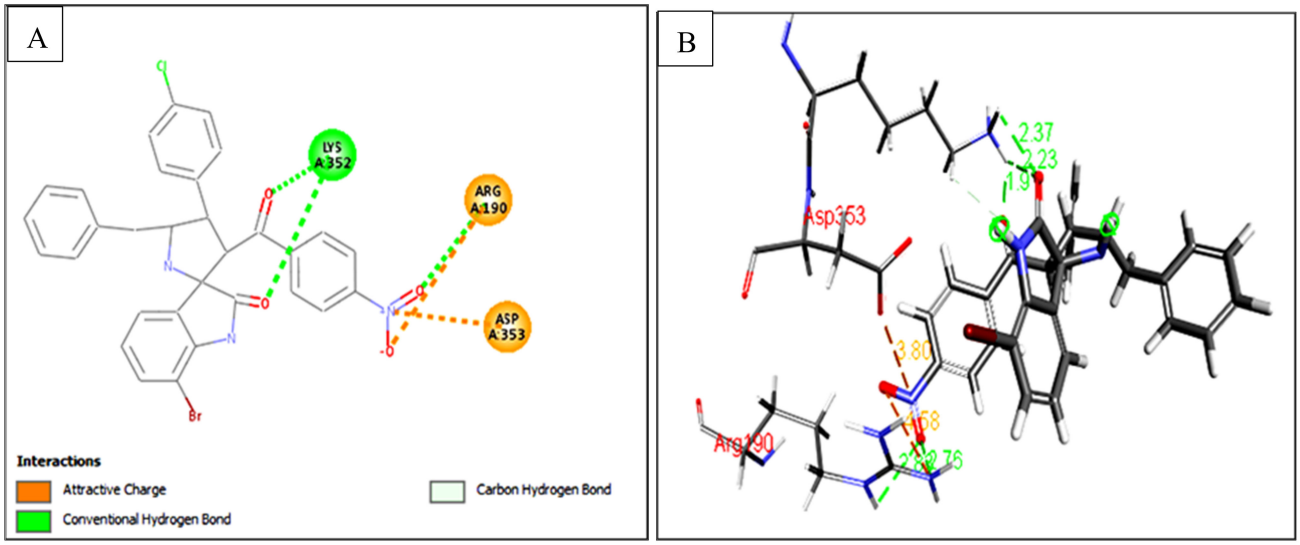

Figure 7. (**A**): Predicted 2D interactions of **24e** with *Leishmania donovani* (PDB ID: 2B9S) with a docking total score of 96.0439, revealing a conventional H-bonding carbonyl group with the amino acid residue, i.e., the side chain of LYS: A-352 (lysine). (**B**) Predicted 3D interactions of **24e** with *Leishmania donovani* (PDB ID: 2B9S) with a docking total score of 96.0439, revealing attractive charge interactions with ASP: A-353 (aspartic acid) and ARG: A-190 (arginine).

Similar to compound **24e**, the docking profile for **24f** against the antileishmanial target showed a docking score of 131.125 and revealed non-bonding Van der Waals interactions with GLU A:182, LYS A:251 (lysine), ASN B:221 (asparagine), THR B:217 (threonine), and TYR B:222 (tyrosine).

The π–anion interaction was observed between LYS A:352 (lysine) and isatin of bond length 3.85 Å. The conventional H-bonding of amino acids ASP: A-353 (aspartic acid) and ARG: A-190 (arginine) with bond lengths of 3.52 Å and 2.43 Å were present along with NH and carbonyl group moieties of ligand **24f**, respectively. Subsequently, **24f** also showed other interactions involving carbon–hydrogen bonds as well as π–cation, π–anion, and π–alkyl interactions (Figure 8).

The docking results for **25d** against *Leishmania donovani* (PDB ID: 2B9S) showed a high binding affinity docking score, indicated by a total score of 83.1911, and it mostly formed nonbonding Van der Waals interactions with amino acid residues GLY: A-189 (glycine), LYS: A-319 (lysine), HIS: A-193 (histidine), PHE: A-187 (phenylalanine), GLN: A-454 (glutamine), THR: B-217 (threonine), ARG: A-314 (arginine), ASN: B-221 (asparagine), ALA: A-324 (alanine), LYS: A-407 (lysine), and LYS: A-269 (lysine). It also shows a π–anion interaction between the phenyl moiety and ASP: A-353 (aspartic acid) and conventional hydrogen bonding between carbonyl oxygen and the amino acid residue, LYS: A-352 (lysine). The pair of alkyl–π–alkyl interactions HIS: A-453 (histidine) with a bond length of 5.24 Å and ARG: A-190 (arginine) with a bond length of 4.91 Å were also present, along with π–π T-shaped TYR: B-222 (thyrosine) with a bond length of 2.97 Å (Figure 9).

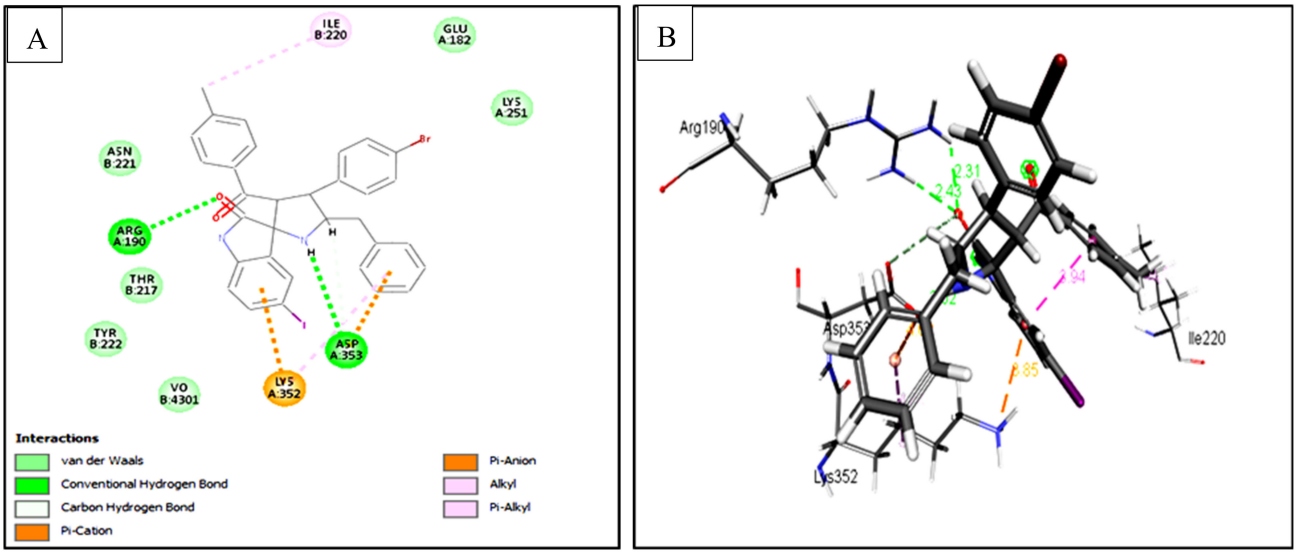

Figure 8. (**A**): Predicted 2D interactions of **24f** with *Leishmania donovani* (PDB ID: 2B9S) with a docking total score of 131.125, giving conventional H-bonding of the carbonyl group with the amino acid residue, i.e., the side chain of LYS: A-352 (lysine). (**B**) Predicted 3D interactions of **24f** with *Leishmania donovani* (PDB ID: 2B9S) with a docking total score of 131.125, revealing conventional H bonding interactions with ASP: A-353 (aspartic acid), and ARG: A-190 (arginine).

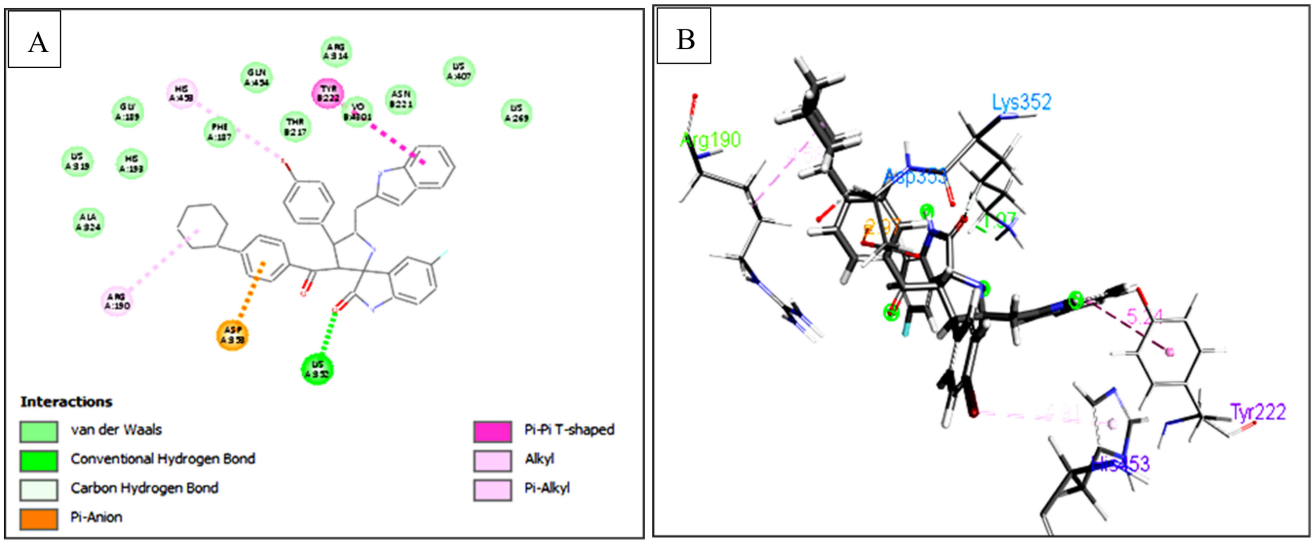

Figure 9. (**A**): Predicted 2D interactions of **25d** with *Leishmania donovani* (PDB ID: 2B9S) with a docking total score of 83.1911, revealing H-bonding to the hydrophobic aliphatic residue, i.e., the side chain of LYS: A-352 (lysine). (**B**) Predicted 3D interactions of **25d** with *Leishmania donovani* (PDB ID: 2B9S) with a docking total score of 83.1911, revealing alkyl–π–alkyl interaction and π–π T-shaped interaction with TYR: B-222 (thyrosine).

The docking results for camptothecin against *Leishmania donovani* showed a high binding affinity docking score indicated by a total score of 123.320 and formed two conventional H-bonds of length 2.55 Å and 1.79 Å to the hydrophobic nucleophilic residues, i.e., the side chains of ALA: A-324 (alanine) and LYS: A-319 (lysine), respectively. In the docking pose of the complex, the chemical nature of binding site residues showed non-bonding Van der Waals interactions with PHE: A-187 (phenylalanine), GLY: A-189 (glycine), THR: A-326 (threonine), SER: A-354 (serine), and GLU: A-353 (glutamic acid), which give extra stability and activity in this compound. In addition, camptothecin also exhibited the π–cation

interaction with ARG: A-190 (arginine) and the alkyl–π–alkyl interaction with ALA: A-324 (alanine) and HIS: A-193 (histidine) amino acid residues (Figure 10).

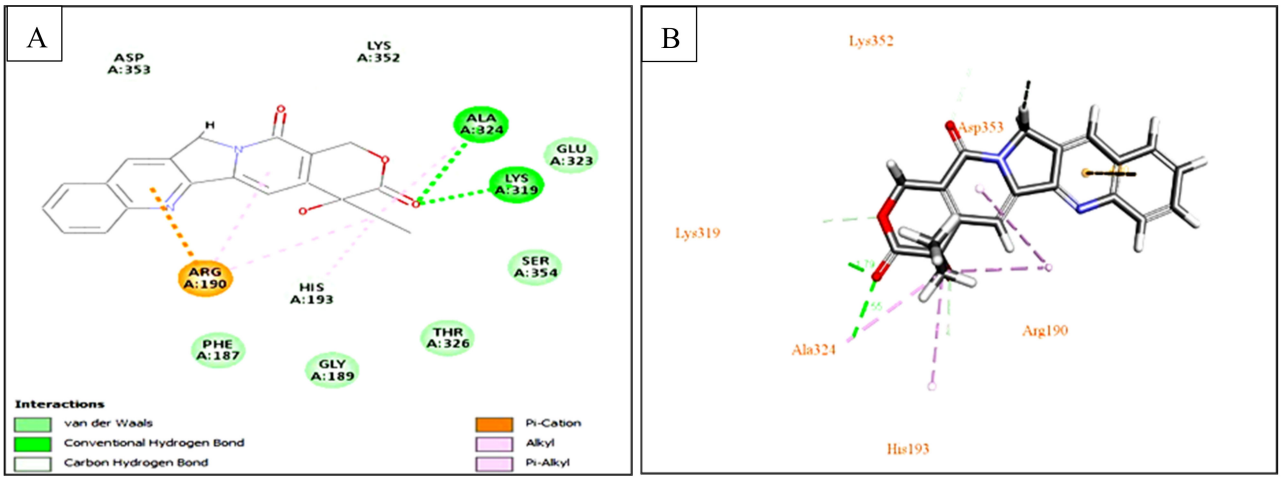

Figure 10. (**A**): Predicted 2D interactions of camptothecin with *Leishmania donovani* (PDB ID: 2B9S) with a docking total score of 123.320, revealing H-bonding to the hydrophobic aliphatic residue, i.e., the side chain of ALA: A-324 (alanine). (**B**) Predicted 3D interactions of camptothecin with *Leishmania donovani* (PDB ID: 2B9S) with a docking total score of 128.598, showing different binding interaction and alkyl–π–alkyl interaction with ARG: A-190 (arginine).

3. Conclusions

In conclusion, we report the microwave-assisted synthesis of a novel series of functionalized spiro[indoline-3,2′-pyrrolidin]-2-one/spiro[indoline-3,3′-pyrrolizin]-2-one derivatives, i.e., **23a–f**, **24a–f**, and **25a–g**, and these have pharmaceutically privileged chalcones and amino acids. The time required for completion of reaction in MM varied from 5 min as compared to CM, which required 3 h. We also report, for the first time, the antileishmanial activity and SAR studies of **23a–f**, **24a–f**, and **25a–g**, which were validated by carrying out molecular docking studies of **24a**, **24e**, **24f**, and **25d**. The stereochemistry of the novel functionalized spiro[indoline-3,2′-pyrrolidin]-2-one/spiro[indoline-3,3′-pyrrolizin]-2-one derivatives were confirmed by single-crystal X-ray crystallography studies of **23f**. Among all the synthesized compounds, **24a** (IC_{50} = 2.43 μM), **24e** (IC_{50} = 0.96 μM), **24f** (IC_{50} = 1.62 μM), and **25d** (IC_{50} = 3.55 μM) showed potent in vitro antileishmanial activity against *Leishmania donovani* in comparison to the standard drug Amphotericin B (IC_{50} = 0.060 μM). All the compounds were tried as potential inhibitors of LTopIB, but only **24a**, **24e**, **24f**, and **25d** were able to inhibit the recombinant enzyme in vitro. Subsequently, the molecular docking studies validated the biological results. In short, our findings qualify the studied molecules as prospective antileishmanial agents with distinct pharmaceutically privileged structures that pave the way for further advanced applications.

Supplementary Materials: The following supporting information can be downloaded at: https://www.mdpi.com/article/10.3390/molecules28124817/s1, Figures S1–S38: ^{1}H NMR and ^{13}C NMR Spectral Data of **23a–f**, **24a–f,** and **25a–g**; Tables S1–S6: X-ray Crystallography: Single-crystal data of spirooxindole **23f**. General experimental conditions; General Procedure for the Synthesis of Chalcones **21a–f**; General Procedure (GP) for the Synthesis of Spirooxindole Derivatives, **23a–f**, **24a–f**, and **25a–g**; Biological Methods**:** Parasite strain and culture conditions, In vitro antileishmanial activity, and Plasmid relaxation assay**;** Characterization data of spirooxindole derivatives (**23a–f**, **24a–f**, **25a–g**); X-ray Crystallography: Single-crystal data of spirooxindole **23f**; optical rotation, ^{1}H and ^{13}C NMR spectral data of all the synthesized compounds **23a–f**, **24a–f** and **25a–g.**

Author Contributions: Conceptualization, S.C.; methodology, N.K.S., R.S. (Ritu Sharma), K.P.S., J.J., K.P. and R.S. (Richa Sharma); software, S.C.; validation, N.K.S., R.S. (Ritu Sharma), K.P.S. and R.S. (Richa Sharma); investigation, S.C., N.K.S., R.S. (Richa Sharma), K.P.S., J.J., K.P., R.S. (Richa Sharma), R.P., S.K., M.J., C.C., X.H. and P.C.; resources, S.C., P.C., C.C. and R.P.; and data curation, N.K.S., R.S. (Ritu Sharma), K.P.S., J.J., K.P., R.S. (Richa Sharma) and X.H.; writing—original draft preparation, S.C.; writing—review and editing, S.C., P.C., N.K.S., R.S. (Richa Sharma), K.P.S. and C.C.; supervision, S.C., P.C., M.J., S.K., R.P. and C.C.; project administration, S.C.; funding acquisition, S.C., P.C., R.P. and C.C. All authors have read and agreed to the published version of the manuscript.

Funding: S.C. acknowledges the funding of this research work from Core Research Grant (CRG), Science and Engineering Research Board (SERB), New Delhi [CRG/2019/005102] and Indian Council of Medical Research (ICMR) Grant, New Delhi [61/8/2O2O-IMM/BMS]. R.P acknowledges the present work which has been partly supported by CSIR, New Delhi Grant No. 02(0286)/16/EMR-II; and ICMR, New Delhi Grant No. BIC/12(03)/2014 for funding. P.C. acknowledges Macau University of Science and Technology and School of Pharmacy (FRG-22-077-SP). This research was funded by the Ministry of Science and Technology in Taiwan, grant numbers MOST 110-2113-M-039-001 and MOST 111-2221-E-039-009 for C.C.

Institutional Review Board Statement: Not applicable.

Informed Consent Statement: Not applicable.

Data Availability Statement: Not applicable.

Acknowledgments: N.K.S acknowledges GEC, Bharatpur, India for providing financial assistance. R.S. (Ritu) and R.S. (Richa) acknowledge MNIT Jaipur for providing institute fellowship. K.P.S. is grateful to the Department of Pharmaceuticals (DoP), Ministry of Chemicals and Fertilizers, Government of India for providing M.S.Pharm Fellowship. J.J. acknowledges Central Council for Research in Homeopathy (CCRH) for providing Research Associateship. R.P. is thankful to the University Science Instrumentation Centre (USIC), University of Delhi for recording the single-crystal X-ray experiments. K.P. thanks to Sanjay Kumar, Technical Assistant (X-ray), USIC, University of Delhi. Materials Research Centre (MRC), MNIT Jaipur and Central instrumentation facility (CIF), NIPER-Raebareli is gratefully acknowledged for providing analytical facilities. The NIPER-Raebareli manuscript communication number is NIPER-R/Communication/419.

Conflicts of Interest: The authors declare no conflict of interest.

Sample Availability: Samples of the compounds will be available from the authors.

References

1. Global Health Observatory. *Leishmaniasis*; World Health Organization: Geneva, Switzerland, 2023. Available online: https://www.who.int/data/gho/data/themes/topics/topic-details/GHO/leishmaniasis (accessed on 12 January 2023).
2. Leishmaniasis Country Profiles; World Health Organization: Geneva, Switzerland. 2023. Available online: https://leishinfowho-cc55.es/country-profiles/ (accessed on 12 January 2023).
3. Mann, S.; Frasca, K.; Scherrer, S.; Henao-Martínez, A.F.; Newman, S.; Ramanan, P.; Suarez, J.A. A Review of Leishmaniasis: Current Knowledge and Future Directions. *Curr. Trop. Med. Rep.* **2021**, *8*, 121–132. [CrossRef] [PubMed]
4. Chappuis, F.; Sundar, S.; Hailu, A.; Ghalib, H.; Rijal, S.; Peeling, R.W.; Alvar, J.; Boelaert, M. Visceral Leishmaniasis: What Are the Needs for Diagnosis, Treatment and Control? *Nat. Rev. Microbiol.* **2007**, *5*, 873–882. [CrossRef] [PubMed]
5. Phumee, A.; Jariyapan, N.; Chusri, S.; Hortiwakul, T.; Mouri, O.; Gay, F.; Limpanasithikul, W.; Siriyasatien, P. Determination of Anti-Leishmanial Drugs Efficacy against Leishmania Martiniquensis Using a Colorimetric Assay. *Parasite Epidemiol. Control.* **2020**, *9*, e00143. [CrossRef] [PubMed]
6. Brindha, J.; Balamurali, M.M.; Chanda, K. An Overview on the Therapeutics of Neglected Infectious Diseases—Leishmaniasis and Chagas Diseases. *Front. Chem.* **2021**, *9*, 622286. [CrossRef]
7. Gonçalves, G.A.; Spillere, A.R.; das Neves, G.M.; Kagami, L.P.; von Poser, G.L.; Canto, R.F.S.; Eifler-Lima, V. Natural and Synthetic Coumarins as Antileishmanial Agents: A Review. *Eur. J. Med. Chem.* **2020**, *203*, 112514. [CrossRef]
8. Leishmaniasis Fact Sheet; World Health Organization: Geneva, Switzerland. 2023. Available online: https://www.who.int/news-room/fact-sheets/detail/leishmaniasis (accessed on 12 January 2023).
9. Jossang, A.; Jossang, P.; Bodo, B.; Hadi, H.A.; Sévenet, T. Horsfiline, an Oxindole Alkaloid from Horsfieldia Superba. *J. Org. Chem.* **1991**, *56*, 6527–6530. [CrossRef]
10. Kulkarni, M.G.; Dhondge, A.P.; Chavhan, S.W.; Borhade, A.S.; Shaikh, Y.B.; Birhade, D.R.; Desai, M.P.; Dhatrak, N.R. Total Synthesis of (±)-Coerulescine and (±)-Horsfiline. *Beilstein J. Org. Chem.* **2010**, *6*, 876–879. [CrossRef]

11. Colegate, S.M.; Anderton, N.; Edgar, J.; Bourke, C.A.; Oram, R.N. Suspected Blue Canary Grass (*Phalaris coerulescens*) Poisoning of Horses. *Aust. Vet. J.* **1999**, *77*, 537–538. [CrossRef]
12. Lee, S.; Yang, J.; Yang, S.; Lee, G.; Oh, D.; Ha, M.W.; Park, H. Enantioselective Synthesis of (+)-Coerulescine by a Phase-Transfer Catalytic Allylation of Diphenylmethyl Tert-Butyl α-(2-Nitrophenyl)Malonate. *Front. Chem.* **2020**, *8*, 577371. [CrossRef]
13. Trost, B.M.; Cramer, N.; Bernsmann, H. Concise Total Synthesis of (±)-Marcfortine B. *J. Am. Chem. Soc.* **2007**, *129*, 3086–3087. [CrossRef]
14. Cui, C.B.; Kakeya, H.; Osada, H. Novel Mammalian Cell Cycle Inhibitors, Spirotryprostatins A and B, Produced by Aspergillus Fumigatus, Which Inhibit Mammalian Cell Cycle at G2/M Phase. *Tetrahedron* **1996**, *52*, 12651–12666. [CrossRef]
15. Cui, C.B.; Kakeya, H.; Osada, H. Spirotryprostatin B, a Novel Mammalian Cell Cycle Inhibitor Produced by Aspergillus Fumigatus. *J. Antibiot.* **1996**, *49*, 832–835. [CrossRef] [PubMed]
16. Pellegrini, C.; Weber, M.; Borschberg, H.-J. Total Synthesis of (+)-Elacomine and (−)-Isoelacomine, Two Hitherto Unnamed Oxindole Alkaloids from Elaeagnus Commutata. *Helv. Chim. Acta* **1996**, *79*, 151–168. [CrossRef]
17. Ban, Y.; Taga, N.; Oishi, T. The Synthesis of 3-Spirooxindole Derivatives. Total Syntheses of Dl-Formosanine, Dl-Isoformosanine, Dl-Mitraphylline and Dl-Isomitraphylline. *Tetrahedron Lett.* **1974**, *15*, 187–190. [CrossRef]
18. Chan, K.C.; Morsingh, F.; Yeoh, G.B. Alkaloids of Uncaria Pteropoda. Isolation and Structures of Pteropodine and Isopteropodine. *J. Chem. Soc. Perkin 1* **1966**, *24*, 2245–2249. [CrossRef]
19. Ghedira, K.; Zeches-Hanrot, M.; Richard, B.; Massiot, G.; Le Men-Olivier, L.; Sevenet, T.; Goh, S.H. Alkaloids of Alstonia Angustifolia. *Phytochemistry* **1988**, *27*, 3955–3962. [CrossRef]
20. Shi, J.-S.; Yu, J.-X.; Chen, X.-P.; Xu, R.-X. Pharmacological Actions of Uncaria Alkaloids, Rhynchophylline and Isorhynchophylline. *Acta Pharmacol. Sin.* **2003**, *24*, 97–101.
21. Lerchner, A.; Carreira, E.M. First Total Synthesis of (±)-Strychnofoline via a Highly Selective Ring-Expansion Reaction. *J. Am. Chem. Soc.* **2002**, *124*, 14826–14827. [CrossRef]
22. Budovská, M.; Kutschy, P.; Kožár, T.; Gondová, T.; Petrovaj, J. Synthesis of Spiroindoline Phytoalexin (S)-(−)-Spirobrassinin and Its Unnatural (R)-(+)-Enantiomer. *Tetrahedron* **2013**, *69*, 1092–1104. [CrossRef]
23. García Prado, E.; García Gimenez, M.D.; De la Puerta Vázquez, R.; Espartero Sánchez, J.L.; Sáenz Rodríguez, M.T. Antiproliferative Effects of Mitraphylline, a Pentacyclic Oxindole Alkaloid of Uncaria Tomentosa on Human Glioma and Neuroblastoma Cell Lines. *Phytomedicine* **2007**, *14*, 280–284. [CrossRef]
24. Kato, H.; Yoshida, T.; Tokue, T.; Nojiri, Y.; Hirota, H.; Ohta, T.; Williams, R.M.; Tsukamoto, S. Notoamides A–D: Prenylated Indole Alkaloids Isolated from a Marine-Derived Fungus, *Aspergillus* sp. *Angew. Chem. Int. Ed.* **2007**, *46*, 2254–2256. [CrossRef] [PubMed]
25. Bhaskar, G.; Arun, Y.; Balachandran, C.; Saikumar, C.; Perumal, P.T. Synthesis of Novel Spirooxindole Derivatives by One Pot Multicomponent Reaction and Their Antimicrobial Activity. *Eur. J. Med. Chem.* **2012**, *51*, 79–91. [CrossRef]
26. Nandakumar, A.; Thirumurugan, P.; Perumal, P.T.; Vembu, P.; Ponnuswamy, M.N.; Ramesh, P. One-Pot Multicomponent Synthesis and Anti-Microbial Evaluation of 2′-(Indol-3-Yl)-2-Oxospiro(Indoline-3,4′-Pyran) Derivatives. *Bioorg. Med. Chem. Lett.* **2010**, *20*, 4252–4258. [CrossRef] [PubMed]
27. Stump, C.A.; Bell, I.M.; Bednar, R.A.; Bruno, J.G.; Fay, J.F.; Gallicchio, S.N.; Johnston, V.K.; Moore, E.L.; Mosser, S.D.; Quigley, A.G.; et al. The Discovery of Highly Potent CGRP Receptor Antagonists. *Bioorg. Med. Chem. Lett.* **2009**, *19*, 214–217. [CrossRef] [PubMed]
28. Girgis, A.S. Regioselective Synthesis of Dispiro [1H-Indene-2,3′-Pyrrolidine-2′,3″-[3H]Indole]-1,2″(1″H)-Diones of Potential Anti-Tumor Properties. *Eur. J. Med. Chem.* **2009**, *44*, 91–100. [CrossRef]
29. Rajanarendar, E.; Ramakrishna, S.; Govardhan Reddy, K.; Nagaraju, D.; Reddy, Y.N. A Facile Synthesis, Anti-Inflammatory and Analgesic Activity of Isoxazolyl-2,3-Dihydrospiro[Benzo[f]Isoindole-1,3′-Indoline]-2′,4,9-Triones. *Bioorg. Med. Chem. Lett.* **2013**, *23*, 3954–3958. [CrossRef]
30. Zinser, E.W.; Wolf, M.L.; Alexander-Bowman, S.J.; Thomas, E.M.; Davis, J.P.; Groppi, V.E.; Lee, B.H.; Thompson, D.P.; Geary, T.G. Anthelmintic Paraherquamides Are Cholinergic Antagonists in Gastrointestinal Nematodes and Mammals. *J. Vet. Pharmacol. Ther.* **2002**, *25*, 241–250. [CrossRef] [PubMed]
31. Rajesh, S.M.; Perumal, S.; Menéndez, J.C.; Yogeeswari, P.; Sriram, D. Antimycobacterial Activity of Spirooxindolo-Pyrrolidine, Pyrrolizine and Pyrrolothiazole Hybrids Obtained by a Three-Component Regio- and Stereoselective 1,3-Dipolar Cycloaddition. *MedChemComm* **2011**, *2*, 626–630. [CrossRef]
32. Ali, M.A.; Ismail, R.; Choon, T.S.; Yoon, Y.K.; Wei, A.C.; Pandian, S.; Kumar, R.S.; Osman, H.; Manogaran, E. Substituted Spiro [2.3′] Oxindolespiro [3.2″]-5,6-Dimethoxy-Indane-1″-One-Pyrrolidine Analogue as Inhibitors of Acetylcholinesterase. *Bioorg. Med. Chem. Lett.* **2010**, *20*, 7064–7066. [CrossRef]
33. Kia, Y.; Osman, H.; Kumar, R.S.; Murugaiyah, V.; Basiri, A.; Perumal, S.; Wahab, H.A.; Bing, C.S. Synthesis and Discovery of Novel Piperidone-Grafted Mono- and Bis-Spirooxindole-Hexahydropyrrolizines as Potent Cholinesterase Inhibitors. *Bioorg. Med. Chem. Lett.* **2013**, *21*, 1696–1707. [CrossRef]
34. Arun, Y.; Saranraj, K.; Balachandran, C.; Perumal, P.T. Novel Spirooxindole-Pyrrolidine Compounds: Synthesis, Anticancer and Molecular Docking Studies. *Eur. J. Med. Chem.* **2014**, *74*, 50–64. [CrossRef] [PubMed]
35. Yu, B.; Yu, D.Q.; Liu, H.M. Spirooxindoles: Promising Scaffolds for Anticancer Agents. *Eur. J. Med. Chem.* **2015**, *97*, 673–698. [CrossRef] [PubMed]

36. Bora, D.; Kaushal, A.; Shankaraiah, N. Anticancer Potential of Spirocompounds in Medicinal Chemistry: A Pentennial Expedition. *Eur. J. Med. Chem.* **2021**, *215*, 113263. [CrossRef]
37. Kornet, M.J.; Thio, A.P. Oxindole-3-Spiropyrrolidines and -Piperidines. Synthesis and Local Anesthetic Activity. *J. Med. Chem.* **1976**, *19*, 892–898. [CrossRef] [PubMed]
38. Jiang, T.; Kuhen, K.L.; Wolff, K.; Yin, H.; Bieza, K.; Caldwell, J.; Bursulaya, B.; Wu, T.Y.-H.; He, Y. Design, Synthesis and Biological Evaluations of Novel Oxindoles as HIV-1 Non-Nucleoside Reverse Transcriptase Inhibitors. Part I. *Bioorg. Med. Chem. Lett.* **2006**, *16*, 2105–2108. [CrossRef] [PubMed]
39. Leañez, J.; Nuñez, J.; García-Marchan, Y.; Sojo, F.; Arvelo, F.; Rodriguez, D.; Buscema, I.; Alvarez-Aular, A.; Serrano-Martín, X. Anti-Leishmanial Effect of Spiro Dihydroquinoline-Oxindoles on Volume Regulation Decrease and Sterol Biosynthesis of Leishmania Braziliensis. *Exp. Parasitol.* **2019**, *198*, 31–38. [CrossRef] [PubMed]
40. Nisbet, L.J.; Moore, M. Will Natural Products Remain an Important Source of Drug Research for the Future? *Curr. Opin. Biotechnol.* **1997**, *8*, 708–712. [CrossRef]
41. Galloway, W.R.J.D.; Isidro-Llobet, A.; Spring, D.R. Diversity-Oriented Synthesis as a Tool for the Discovery of Novel Biologically Active Small Molecules. *Nat. Commun.* **2010**, *1*, 80. [CrossRef]
42. Yousuf, M.; Mukherjee, D.; Dey, S.; Chatterjee, S.; Pal, A.; Sarkar, B.; Pal, C.; Adhikari, S. Synthesis and Biological Evaluation of Polyhydroxylated Oxindole Derivatives as Potential Antileishmanial Agent. *Bioorg. Med. Chem. Lett.* **2018**, *28*, 1056–1062. [CrossRef]
43. Saha, S.; Acharya, C.; Pal, U.; Chowdhury, S.R.; Sarkar, K.; Maiti, N.C.; Jaisankar, P.; Majumder, H.K. A Novel Spirooxindole Derivative Inhibits the Growth of *Leishmania donovani* Parasites Both in Vitro and in Vivo by Targeting Type IB Topoisomerase. *Antimicrob. Agents Chemother.* **2016**, *60*, 6281–6293. [CrossRef]
44. Paul Chowdhuri, S.; Dhiman, S.; Das, S.K.; Meena, N.; Das, S.; Kumar, A.; Brata Das, B. Novel Pyrido[2′,1′:2,3]Imidazo[4,5-c]Quinoline Derivative Selectively Poisons *Leishmania donovani* Bisubunit Topoisomerase 1 to Inhibit the Antimony-Resistant Leishmania Infection in Vivo. *J. Med. Chem.* **2023**, *66*, 3411–3430. [CrossRef] [PubMed]
45. Pathan, S.; Singh, G.P. Synthesis of Novel Tetrazole Tetrahydrobenzo[b]Thiophene via Ugi-MCR: As New Antileishmanial Prototype. *J. Saudi Chem. Soc.* **2021**, *25*, 101295. [CrossRef]
46. Scala, A.; Cordaro, M.; Grassi, G.; Piperno, A.; Barberi, G.; Cascio, A.; Risitano, F. Direct Synthesis of C3-Mono-Functionalized Oxindoles from N-Unprotected 2-Oxindole and Their Antileishmanial Activity. *Bioorg. Med. Chem. Lett.* **2014**, *22*, 1063–1069. [CrossRef] [PubMed]
47. Altowyan, M.S.; Atef, S.; Al-Agamy, M.H.; Soliman, S.M.; Ali, M.; Shaik, M.R.; Choudhary, M.I.; Ghabbour, H.A.; Barakat, A. Synthesis and Characterization of a Spiroindolone Pyrothiazole Analog via X-ray, Biological, and Computational Studies. *J. Mol. Struct.* **2019**, *1186*, 384–392. [CrossRef]
48. Almeida, F.S.; Sousa, G.L.S.; Rocha, J.C.; Ribeiro, F.F.; de Oliveira, M.R.; de Lima Grisi, T.C.S.; Araújo, D.A.M.; Michelangela, M.S.; Castro, R.N.; Amaral, I.P.G.; et al. In Vitro Anti-Leishmania Activity and Molecular Docking of Spiro-Acridine Compounds as Potential Multitarget Agents against Leishmania Infantum. *Bioorg. Med. Chem. Lett.* **2021**, *49*, 128289. [CrossRef] [PubMed]
49. Mohamed, M.A.A.; Kadry, A.M.; Bekhit, S.A.; Abourehab, M.A.S.; Amagase, K.; Ibrahim, T.M.; El-Saghier, A.M.M.; Bekhit, A.A. Spiro Heterocycles Bearing Piperidine Moiety as Potential Scaffold for Antileishmanial Activity: Synthesis, Biological Evaluation, and in Silico Studies. *J. Enzym. Inhib. Med. Chem.* **2023**, *38*, 330–342. [CrossRef]
50. de la Hoz, A. Microwave Heating as a Tool for Sustainable Chemistry. Edited by Nicholas E. Leadbeater. *ChemSusChem* **2011**, *4*, 666. [CrossRef]
51. Luu, T.X.T.; Lam, T.T.; Le, T.N.; Duus, F. Fast and Green Microwave-Assisted Conversion of Essential Oil Allylbenzenes into the Corresponding Aldehydes via Alkene Isomerization and Subsequent Potassium Permanganate Promoted Oxidative Alkene Group Cleavage. *Molecules* **2009**, *14*, 3411–3424. [CrossRef]
52. Polshettiwar, V.; Nadagouda, M.N.; Varma, R.S. Microwave-Assisted Chemistry: A Rapid and Sustainable Route to Synthesis of Organics and Nanomaterials. *Aust. J. Chem.* **2009**, *62*, 16–26. [CrossRef]
53. Suna, E.; Mutule, I. Microwave-assisted Heterocyclic Chemistry. In *Microwave Methods in Organic Synthesis*; Larhed, M., Olofsson, K., Eds.; Topics in Current Chemistry; Springer: Berlin, Germany, 2006; Volume 266, pp. 49–101. [CrossRef]
54. Kappe, C.O.; Dallinger, D.; Murphree, S.S. *Practical Microwave Synthesis for Organic Chemists: Strategies, Instruments, and Protocols*; John Wiley Sons: New York, NY, USA, 2009; pp. 1–299. [CrossRef]
55. Kumar, S.; Prince; Gupta, M.; Lalji, R.S.K.; Singh, B.K. Microwave assisted regioselective halogenation of benzo[b][1,4]oxazin-2-ones via sp2 C–H functionalization. *RCS Adv.* **2023**, *13*, 2365–2371. [CrossRef]
56. Gawande, M.B.; Shelke, S.N.; Zboril, R.; Varma, R.S. Microwave-Assisted Chemistry: Synthetic Applications for Rapid Assembly of Nanomaterials and Organics. *Acc. Chem. Res.* **2014**, *47*, 1338–1348. [CrossRef] [PubMed]
57. Huisgen, R.; Padwa, A. *1 3-Dipolar Cycloaddition Chemistry*; Wiley: New York, NY, USA, 1984; Volume 1, pp. 55–92.
58. Haddad, S.; Boudriga, S.; Akhaja, T.N.; Raval, J.P.; Porzio, F.; Soldera, A.; Askri, M.; Knorr, M.; Rousselin, Y.; Kubicki, M.M.; et al. A Strategic Approach to the Synthesis of Functionalized Spirooxindole Pyrrolidine Derivatives: In Vitro Antibacterial, Antifungal, Antimalarial and Antitubercular Studies. *New J. Chem.* **2015**, *39*, 520–528. [CrossRef]
59. Coldham, I.; Hufton, R. Intramolecular Dipolar Cycloaddition Reactions of Azomethine Ylides. *Chem. Rev.* **2005**, *105*, 2765–2810. [CrossRef]

60. Pandey, G.; Banerjee, P.; Gadre, S.R. Construction of Enantiopure Pyrrolidine Ring System via Asymmetric [3+2]-Cycloaddition of Azomethine Ylides. *Chem. Rev.* **2006**, *106*, 4484–4517. [CrossRef] [PubMed]
61. Gothelf, K.V.; Jørgensen, K.A. Asymmetric 1,3-Dipolar Cycloaddition Reactions. *Chem. Rev.* **1998**, *98*, 863–910. [CrossRef]
62. Lashgari, N.; Ziarani, G.M. Synthesis of Heterocyclic Compounds Based on Isatin through 1,3-Dipolar Cycloaddition Reactions. *Arkivoc* **2012**, *2012*, 277–320. [CrossRef]
63. Rajesh, R.; Raghunathan, R. Regio- and Stereoselective Synthesis of Novel Tetraspiro-Bispyrrolidine and Bisoxindolopyrrolidine Derivatives through 1,3-Dipolar Cycloaddition Reaction. *Tetrahedron Lett.* **2010**, *51*, 5845–5848. [CrossRef]
64. Panda, S.S.; Aziz, M.N.; Stawinski, J.; Girgis, A.S. Azomethine Ylides—Versatile Synthons for Pyrrolidinyl-Compounds. *Molecules* **2023**, *28*, 668. [CrossRef]
65. Abdel-Mohsen, S.A.; Hussein, E.M. A Green Synthetic Approach to the Synthesis of Schiff Bases from 4-Amino-2-Thioxo-1,3-Diazaspiro[5.5]Undec-4-Ene-5-Carbonitrile as Potential Anti-Inflammatory Agents. *Russ. J. Bioorg. Chem.* **2014**, *40*, 343–349. [CrossRef]
66. Mali, P.R.; Chandrasekhara Rao, L.; Bangade, V.M.; Shirsat, P.K.; George, S.A.; Jagadeesh babu, N.; Meshram, H.M. A Convenient and Rapid Microwave-Assisted Synthesis of Spirooxindoles in Aqueous Medium and Their Antimicrobial Activities. *New J. Chem.* **2016**, *40*, 2225–2232. [CrossRef]
67. Dolomanov, O.V.; Bourhis, L.J.; Gildea, R.J.; Howard, J.A.K.; Puschmann, H. OLEX2: A Complete Structure Solution, Refinement and Analysis Program. *J. Appl. Crystallogr.* **2009**, *42*, 339–341. [CrossRef]
68. Wolff, S.K.; Grimwood, D.J.; McKinnon, J.J.; Turner, M.J.; Jayatilaka, D.; Spackman, M.A. *Crystal Explorer 3.0*; University of Western Australia: Perth, Australia, 2012.
69. Sundar, S.; Chakravarty, J.; Agarwal, D.; Rai, M.; Murray, H.W. Single-Dose Liposomal Amphotericin B for Visceral Leishmaniasis in India. *N. Engl. J. Med. Orig.* **2010**, *362*, 504–512. [CrossRef]
70. Champoux, J.J. DNA Topoisomerases: Structure, Function, and Mechanism. *Annu. Rev. Biochem.* **2001**, *70*, 369–413. [CrossRef] [PubMed]
71. Kaur, G.; Chauhan, K.; Kaur, S. Immunotherapeutic Potential of Codonopsis Clematidea and Naringenin against Visceral Leishmaniasis. *Biomed. Pharmacother.* **2018**, *108*, 1048–1061. [CrossRef] [PubMed]
72. Pérez-Pertejo, Y.; Escudero-Martínez, J.M.; Reguera, R.M.; Balaña-Fouce, R.; García, P.A.; Jambrina, P.G.; San, A.; Castro, M-A. Antileishmanial Activity of Terpenylquinones on Leishmania Infantum and Their e Ff Ects on Leishmania Topoisomerase IB. *Int. J. Parasitol. Drugs Drug Resist.* **2019**, *11*, 70–79. [CrossRef]
73. Sharma, G.; Chowdhury, S.; Sinha, S.; Majumder, H.K.; Kumar, S.V. Antileishmanial Activity Evaluation of Bis-Lawsone Analogs and DNA Topoisomerase-I Inhibition Studies. *J. Enzym. Inhib. Med. Chem.* **2014**, *6366*, 185–189. [CrossRef] [PubMed]